Volume 10 | Number 9 | 7 March 2014 | Pages 1235–1430

Soft Matter

www.softmatter.org

ISSN 1744-683X

ROYAL SOCIETY OF CHEMISTRY

PAPER
Michael D. Dickey, Orlin D. Velev *et al.*
Electro-actuated hydrogel walkers with dual responsive legs

Soft Matter

PAPER

View Article Online
View Journal | View Issue

Cite this: *Soft Matter*, 2014, **10**, 1337

Electro-actuated hydrogel walkers with dual responsive legs†

Daniel Morales, Etienne Palleau, Michael D. Dickey* and Orlin D. Velev*

Stimuli responsive polyelectrolyte hydrogels may be useful for soft robotics because of their ability to transform chemical energy into mechanical motion without the use of external mechanical input. Composed of soft and biocompatible materials, gel robots can easily bend and fold, interface and manipulate biological components and transport cargo in aqueous solutions. Electrical fields in aqueous solutions offer repeatable and controllable stimuli, which induce actuation by the re-distribution of ions in the system. Electrical fields applied to polyelectrolyte-doped gels submerged in ionic solution distribute the mobile ions asymmetrically to create osmotic pressure differences that swell and deform the gels. The sign of the fixed charges on the polyelectrolyte network determines the direction of bending, which we harness to control the motion of the gel legs in opposing directions as a response to electrical fields. We present and analyze a walking gel actuator comprised of cationic and anionic gel legs made of copolymer networks of acrylamide (AAm)/sodium acrylate (NaAc) and acrylamide/quaternized dimethylaminoethyl methacrylate (DMAEMA Q), respectively. The anionic and cationic legs were attached by electric field-promoted polyion complexation. We characterize the electro-actuated response of the sodium acrylate hydrogel as a function of charge density and external salt concentration. We demonstrate that "osmotically passive" fixed charges play an important role in controlling the bending magnitude of the gel networks. The gel walkers achieve unidirectional motion on flat elastomer substrates and exemplify a simple way to move and manipulate soft matter devices and robots in aqueous solutions.

Received 14th July 2013
Accepted 19th September 2013

DOI: 10.1039/c3sm51921j

www.rsc.org/softmatter

Introduction

This paper describes the fabrication and characterization of millimeter-scale gel walkers that undergo directional motion in response to electric fields in solution. Robots built from soft matter draw inspiration from the versatile mobility of soft organisms, such as octopi, slugs, and inchworms. Developing simple methods to produce soft actuator devices will enable their use for situations where conventional robotics are inefficient or inadequate, such as handling fragile objects or navigating dynamic, shifting terrain.[1] Elastomeric polymer networks are an ideal soft material for such applications due to the similarity of their mechanical properties to natural tissues.[1,2] Here, we show it is possible to create a walker by binding legs of two types of polyelectrolyte hydrogels that deform in opposite directions in response to an electric field, which allows for locomotion across flat surfaces. We characterize the fundamental properties of these gels to identify the most responsive conditions to induce quick actuation.

Stimuli responsive polyelectrolyte hydrogels are of interest in the area of soft robotics because of their ability to transduce various environmental stimuli into mechanical motion, especially in aqueous environment, without the use of external mechanical actuation. Due to their mostly aqueous, biocompatible matrix, hydrogel-based actuators have the ability to exchange matter and energy with aqueous environments and can manipulate and interface with biological components.[3] The gel networks can be functionalized easily to respond to analytes in solution, enabling the possibility to incorporate actuating, sensing/signaling, transport/release and homeostatic capabilities.[4,5] Additionally, hydrogel networks can be pre-patterned for directional actuation in response to the environment.[6,7] Hence, controlled hydrogel motion has potential uses for understanding soft organism motility, drug delivery, bio detection and environmental sensing. Several examples of biomimetic motion by responsive hydrogels include actuators that respond to temperature,[5,8,9] magnetic fields,[4] pH changes,[10] substrate vibration,[11] elastic instabilities[12] and muscle cell contraction.[13] Autonomously moving gels have been actuated and simulated using the oscillating Belousov–Zhabotinsky reaction, which induces shrinking or swelling in specific regions of the gel network.[14–16]

Department of Chemical and Biomolecular Engineering, North Carolina State University, Raleigh, NC 27695-7905, USA. E-mail: mddickey@ncsu.edu; odvelev@ncsu.edu

† Electronic supplementary information (ESI) available. See DOI: 10.1039/c3sm51921j

Stimulating the motion of hydrogels using external electrical fields is appealing due to the reliable control of the signal strength and direction. This stimulus only requires ions to be present in the external solution to induce actuation. Electrical fields applied to polyelectrolyte networks submerged in electrolyte solution distribute the mobile ions asymmetrically to create osmotic pressure differences that swell and deform the gel. These physical and chemical processes are analogous to those of mobile ion exchange between a cell membrane and its environment. Common processes in nature, including photosynthesis, cell respiration, signal transmission by nerve excitation, and muscle contraction, rely on the exchange of ions to generate osmotic and electrical variations across a membrane.[17] The same process is used in soft robotics applications, where electric fields create osmotic pressure gradients that control the contraction and swelling of the hydrogel.[3,4,18–21] For instance, swimming hydrogels have been demonstrated using electric fields to cause a polyvinyl alcohol/polyacrylic acid gel tail attached to a plastic body to flap in response to a sinusoidally varied electric field.[21] Micro-gel robots resembling octopi and sperm have been achieved by using an asymmetric control signal to bind surfactant from an external solution to the ionized backbone of the gel appendages resulting in unidirectional motion.[4] Although walking function has been demonstrated, unidirectional motion on a substrate has yet to be achieved without extreme electric fields or external parts.[3,4,20]

We sought to create soft walkers from hydrogels that move in common water environments and do not rely on specific external conditions or ratcheted surfaces.[4,11,14,18,22] Looking to nature, we mimic mobility mechanisms utilized by earthworms and inchworms to develop directional movement by a mechanical motion and asymmetric friction.[8,9] To this end, the directional motion in our system originates from gel appendages that deform in opposite directions in response to external stimuli. This motion is realized using gels with opposite charges fixed onto the backbone of the polymers that comprise the gels. The anionic and cationic legs are composed of acrylamide (AAm)/sodium acrylate (NaAc) copolymer and acrylamide/quaternized dimethylaminoethyl methacrylate (DMAEMA-Q) copolymer, respectively. Creating an efficient gel walker using these materials requires (1) developing a method to permanently bond these two networks together, and (2) identifying the appropriate gel composition to optimize the response to electric fields. We describe gel walkers composed of adhered cationic and anionic networks, submerged in salt solutions, which are actuated by modest electric fields (5 V cm^{-1}) and are able to walk on flat, untreated substrates composed of polydimethylsiloxane (PDMS).

Results and discussion

Gel walker fabrication and assembly

The unidirectional motion of the gel walker was achieved by including two appendages that respond differently to the electric field. To confirm the direction of bending, we conducted electro-actuation experiments of the anionic and cationic networks of equimolar composition equilibrated in 0.01 M NaCl. A 20% anionic 2 mm diameter cylinder-shaped gel bends toward the cathode in aqueous NaCl since the pH was well above the $pK_a \sim 4.8$ and the carboxylic groups were ionized (Fig. 1(a)). However, a 20% DMAEMA gel did not respond in aqueous NaCl since its network requires low pH conditions to form ionized tertiary amine groups.[23] To create walkers that are fully ionized at neutral conditions, we replaced DMAEMA with quaternized DMAEMA monomer which results in bending toward the anode (Fig. 1(a)). The bending curvature as a function of time obtained for those gel cylinders is reported in Fig. 1(b) (see ESI for more details†).

The next step was to design the shape of each leg considering the mechanical contact the leg will make with the substrate and the initial angle of contact. Millimeter sized "leg"-shaped pieces were cut from bulk gels using a laser writer as shown in Fig. 2(a).

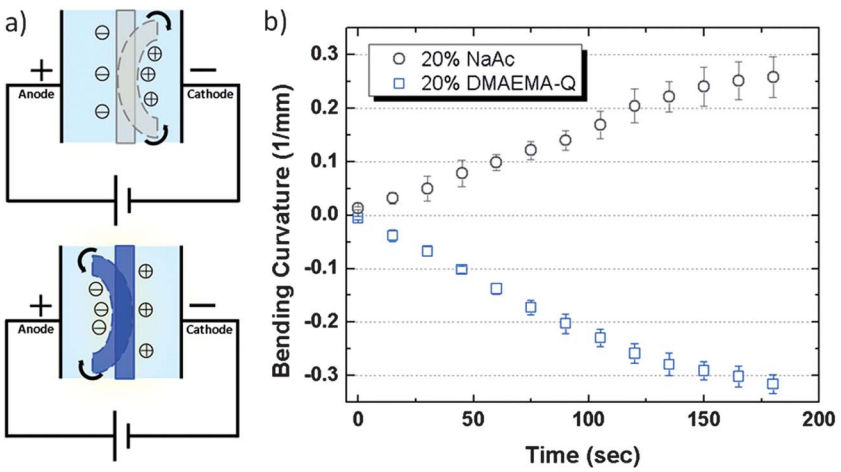

Fig. 1 Overview of the direction of gel bending in electrolyte solution in response to an electric field. (a) Illustrations of the bending direction for gel networks equilibrated in NaCl solutions as a function of the sign of the fixed charge groups (anionic on the top, cationic on the bottom). (b) Graph of the inverse radius of curvature ($1/R$ = bending curvature) as a function of time. Positive curvature indicates bending toward the cathode and negative curvature indicates bending toward the anode.

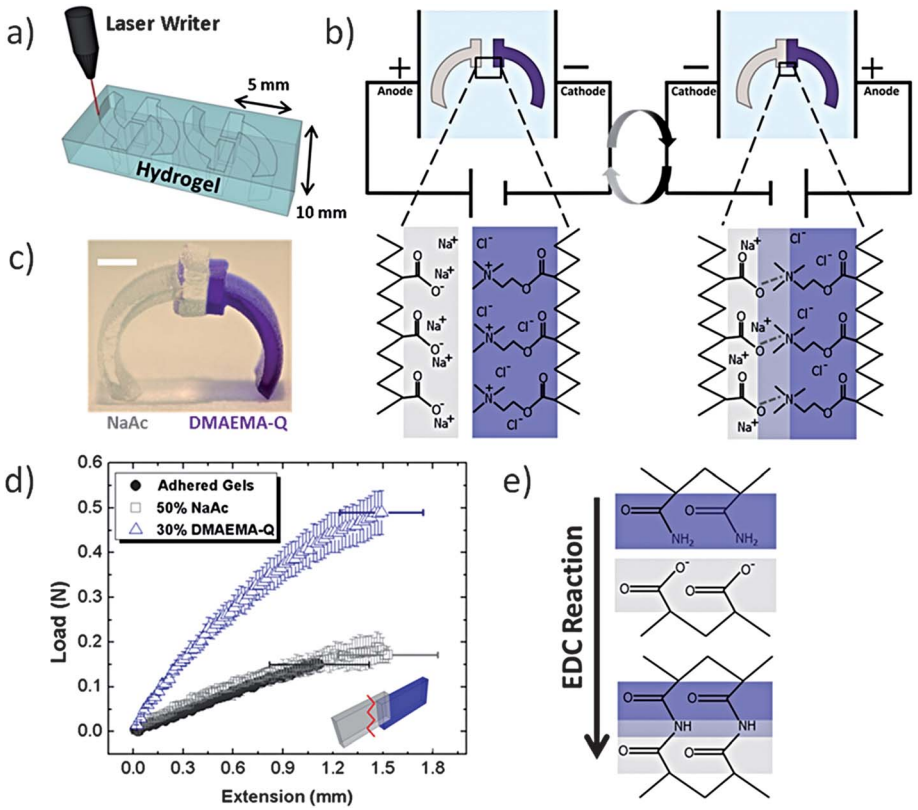

Fig. 2 Overview of the gel walker fabrication process. (a) Illustration of the laser cutting process for creating hydrogel appendages. (b) Electric field assisted adhesion of the oppositely charged gel networks. When charged gel chains cross the cationic/anionic gel interface to move toward their oppositely charged electrode, strong polyion complexes promote adhesion. Reversing the electric field direction separates the gels. (c) Photograph of a finished gel walker. Scale bar = 2.5 mm. (d) Plot of the mechanical load as a function of extension for individual cationic and anionic networks and electro adhered networks. Once adhered, the anionic network breaks instead of the bound interface during extension. (e) Illustration of the *N*-(3-dimethylaminopropyl)-*N*′-ethylcarbodiimide hydrochloride (EDC) reaction between the carboxylic groups and primary amine groups used to promote covalent bonding at the interface between the gel legs.

One technical bottleneck was to attach the two gel legs together without affecting their responsiveness. It is known that hydrogels can adhere in contact with each other or other functionalized surfaces due to hydrogen bonding and hydrophobic side chain interactions.[24–27] Reversible, self-healing hydrogels have been realized by controlling the pH to promote hydrophobic/hydrophilic side chain interactions at the gel interface.[24] However, that method is not applicable here, since the self-healing only occurs at low pH. We utilized a simple, rapid method for reversibly binding hydrogels by promoting electrostatic interactions in solution, originally developed by Kikuchi *et al.*[28,29] The electrostatic polyion complexation at the interface of the two gels in an electrolyte solution is promoted by using electric fields. This technique has the advantage of enabling arbitrary shapes to be reversibly bound to each other as shown in Fig. 2(b) (see also Video 1†). An example of a gel walker after binding the two legs is pictured in Fig. 2(c).

We characterized the strength of adhesion between the oppositely charged gel surfaces. Hydrogel network surfaces are hydrophilic or hydrophobic depending on their environment since the surface chains have enough mobility to minimize their surface energy.[30] Consequently, in water, the hydroxide groups and quaternary amine groups are exposed to the surface and one would expect the two oppositely charge hydrogel networks to attract each other. Indeed we calculated the lap shear adhesion strength between a 50% NaAc and 30% DMAEMA-Q gel simply placed in contact as 6.09 ± 0.97 kPa. After applying an electric field for just a few seconds, the interface becomes stronger than the NaAc gel itself as shown in Fig. 2(d). The strong polyion complexation is due to the high density of charge groups along the polymer backbone. The binding lasts over 24 hours if the two bound gels are left in deionized water. However, in salt solution, the polyionic binding lasts on the order of minutes to hours due to de-shielding of the ionic interactions. Thus, instead we promoted covalent amide bonding at the interface between the carboxylic groups in the NaAc gel and primary amine groups present in the DMAEMA-Q gel by immersion in *N*-(3-dimethylaminopropyl)-*N*′-ethylcarbodiimide hydrochloride (EDC) solution as schematically shown in Fig. 2(d). This reaction provides stable, non-reversible adhesion of the interface when submerged in salt solution and under an electric field. Amide bond formation was not observed within the individual networks themselves after immersion in EDC (see ESI for more details†).

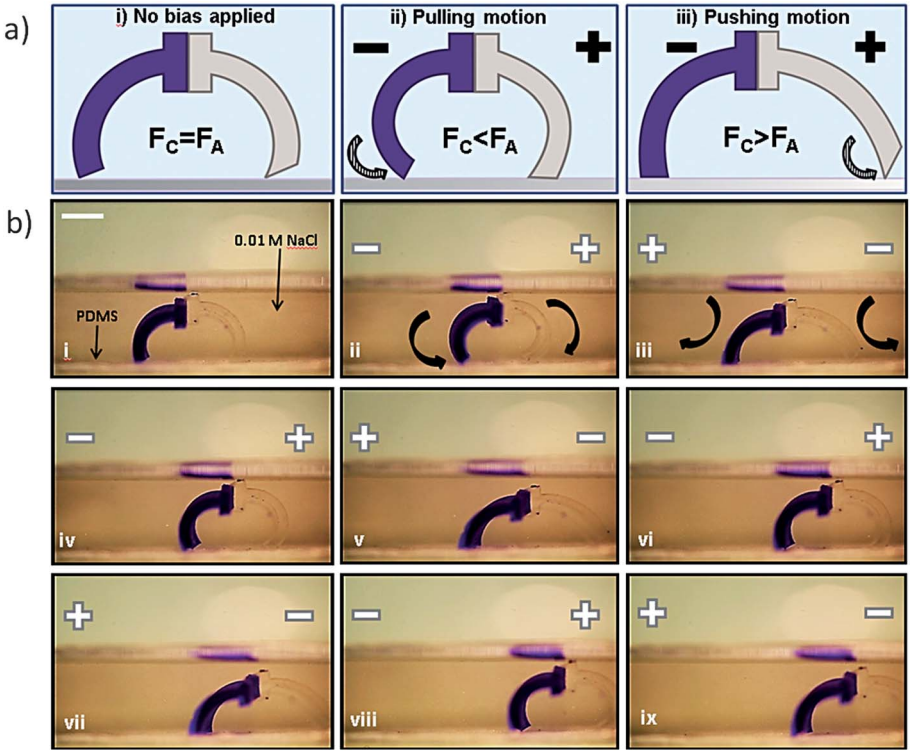

Fig. 3 Actuation mechanism of the gel walker. (a) Illustrations depicting the two modes of actuation depending on the direction of the applied electric field. F_c and F_a are the friction force of the cationic leg (dark blue) and anionic leg (light grey) respectively. (b) Photographs of a gel walker in 0.01 M NaCl composed of 50% NaAc and 30% DMAEMA-Q legs with an applied field of 5 V cm^{-1}. Scale bar = 5 mm.

Gel walker motion mechanism

The walking mechanism involves a delicate interplay between the response rate of the gel appendages and the frequency at which the electric field is reversed (Fig. 3(a)). We characterized the deformation of the sodium polyacrylate networks in response to electric fields (discussed herein) and identified 50% NaAc gels equilibrated in 0.01 M NaCl as the most responsive and thus, best suited for the soft walker robot. We utilized 30% DMAEMA-Q as a second hydrogel to ensure that the legs bent at different directions upon application of the electric field. We also sought to increase the friction between the DMAEMA-Q gels and the PDMS substrate by tuning its mechanical properties to promote asymmetric anchoring. Towards this goal, we tuned the amount of crosslinker used to polymerize the DMAEMA-Q networks (see ESI for more details†). The modulus of the gel increases with a higher degree of crosslinking because the stress is redistributed to a larger number of points within the network.[31] The friction force also increases due to the decrease of the hydrodynamic lubrication layer with a decreasing pore size caused by the higher crosslinker content.[32]

After bonding the anionic/cationic gel appendages in EDC, gel walkers were equilibrated in 0.01 M NaCl solutions. The gel walker was placed on a PDMS substrate in a glass vessel with graphite electrodes placed 6 cm apart. After submerging the gel walker in 0.01 M NaCl solution within the vessel, a video camera recorded the motion while externally controlling the direction of the electric field (5 V cm^{-1}). Fig. 3(b) presents a sequence of images illustrating the motion and Video 2† illustrates the gel walking in aqueous solution.

The sequence of applying the electric field is important for actuating continuous motion. Initially, the field is applied in the direction where the cationic and anionic networks face the cathode and anode, respectively. This field causes the legs to bend inward toward each other. The anionic leg (light grey) has a larger surface area in contact with the PDMS than the cationic leg (Fig. 3(b-i)) and thus pulls the walker to the right. Reversing the field causes the anionic leg to stretch toward the cathode due to the higher friction force of the DMAEMA-Q gel leg, which anchors it on the PDMS substrate (Fig. 3(b-ii)). Thus, the cationic leg effectively pushes the gel walker forward. This cycle continues periodically to enable unidirectional motion on flat surfaces. The largest propulsion velocity achieved was ~2.5 mm min^{-1}. As demonstrated in Video 3,† multiple walkers can be actuated at the same time with identical response to the electrical field.

Electro-actuation

We sought to understand the fundamentals of the mechanism of the hydrogel electro-response as a function of the fixed charge density (mole fraction of charged units in the network) of the sodium acrylate-*co*-acrylamide networks and external electrolyte concentration to maximize the responsiveness of the gel walkers. The extent of differential hydrogel swelling and bending in response to an electric field depends on the polymer

concentration, crosslinking density, charge density and external electrolyte concentration.[33–43] The hydrogel bending at initial time steps is governed by the initial concentrations of mobile ions in the gel C_i^g and in the external solution C_i^s which are related by Donnan equilibrium.[36,40] The fixed charges on the polymer backbone induce a chemical gradient between the mobile ions at the gel/solution interface.[44] Consequently, when an anionic network is placed in salt solution, Donnan equilibrium is established after mobile cations redistribute between the gel and the surrounding solution to maintain electroneutrality and establish equal chemical potential between the phases. This equilibrium results in a higher overall concentration of mobile ions in the gel. Applying an external electric field causes mobile cations to migrate preferentially toward the cathode due to the gel permselectivity (preferential permeation of specific ionic species through hydrated polymer networks) to cations. A higher amount of mobile ions migrate to the side of the gel closest to the cathode and hence the osmotic pressure at the interface of the gel closest to the anode, π_1, becomes larger than that at the cathode interface, π_2.[35,37,39,43] The osmotic contribution from this equilibrium is given by the equation below:

$$\pi_{\text{ion}} = RT \sum_i \left(C_i^{\text{g}} - C_i^{\text{s}}\right) \quad (1)$$

$$\Delta\pi_{\text{ion}} = \pi_1 - \pi_2 \quad (2)$$

A pressure difference of $\Delta\pi_{\text{ion}} > 0$ bends the gel toward the cathode as shown in Fig. 4(a). The opposite behavior is observed for cationic gel networks where $\Delta\pi_{\text{ion}} < 0$.[41,45,46] Indeed, in all electrolyte solutions (0.01 M, 0.05 M and 0.1 M NaCl) the equilibrated anionic gels bent toward the cathode. Negligible bending of the gels occurred in water due to an insufficient amount of mobile counterions.

To investigate eqn (1) experimentally, we conducted gel bending studies on 2 mm diameter gel cylinders as a function of external salt concentration and fixed charge density. The bending curvature ($1/R$) as a function of time for each hydrogel composition is plotted in Fig. 4(b). First, we examined the role of the external salt concentration on the hydrogel bending. An increase of the external salt concentration (from the black to the blue curves) leads to a decrease in osmotic pressure at the hydrogel/solution interface. Higher external salt content diminishes the difference between C_i^g and C_i^s and consequently imposes a smaller driving force for bending. Interestingly, as the fixed charge density increases, the magnitude of bending becomes less sensitive to the external salt concentration (Fig. 4(b)–(i)). This behavior is most likely due to the concentration of mobile ions in the hydrogel network approaching that of the external solution so that during equilibration the amount of ions exchanged between the gel in solution is minute. It is also possible that in such an ion-rich environment, the highly screened ionic interactions decrease the sensitivity of the gel to the external field.[47]

Second, we studied the change in bending magnitude with increased fixed charge density by varying the composition of the ratio of NaAc to AAm in the gel. The nonionic gel (100% AAm) exhibited negligible bending in all solutions within the experimental time, as expected.[35,48,49] Surprisingly, increasing the internal fixed charge density above 70% NaAc does not lead to a monotonic increase in bending rate. The decrease in bending rate while increasing the fixed charge density from 70% to 100% may be due to the emergence of 'osmotically passive' charge groups. These are ionizable, but not effectively ionized, groups that but do not contribute to osmotic swelling due to steric interference, counterion condensation, hydrogen bonding or inhomogeneous electric potential wells within the gel network.[50–54] To the best of our knowledge, the effect of counterion condensation has not been previously taken into account to characterize hydrogel electro-actuation and will be discussed further in the next section.

To achieve rapid actuation, we selected the optimized gel composition based on results from Fig. 5. The bending curvature increased linearly with time during the first minute for each gel sample in Fig. 4(b)–(i). The slope is plotted in Fig. 5 as a function of NaAc content to determine the fastest bending rate The best rate is obtained with 50% NaAc gels in dilute 0.01 M NaCl solutions, which we used for the gel walkers (*cf.* Fig. 2). Other studies report a similar trend where a maximum bending behavior of gels is observed at a critical ratio of fixed charge groups to external ionic solution concentration.[40] Of note is the trend from 80% to 100% NaAc in which the bending in 0.05 M NaCl becomes more pronounced until maximum bending is achieved for the 100% NaAc gel in 0.05 M NaCl as opposed to 0.01 M NaCl (Fig. 4(i) and 5). It appears that regardless of the type of gel, there exists a specific salt concentration that can maximize the gel bending, which depends on the exact number of osmotically active fixed charge groups within the gel. The bending rate of ionic gel networks in response to electric fields is the result of a dynamic interplay between the amount of ionized fixed charges, the distribution of the mobile ions at the hydrogel/solution interface and the effect of the mobilized ions on the state of ionization and electrostatic interactions within the network. The bending mechanism becomes even more complex when electro-actuation experiments are conducted far from equilibrium in a solution containing a much higher salt content than the solution in which the gel was equilibrated.[43] For example, we observed that the initial bending direction of the hydrogels reverses toward the anode when the electro actuation experiments are conducted in 0.1 M NaCl solutions after equilibration in 0.01 M NaCl solutions (See ESI for more details).

Charge density analysis

After observing that the bending rate does not maximize at the highest concentration of NaAc groups, we hypothesized that some of the groups may not be contributing to the actuation (*i.e.*, not contributing to the osmotic effects). We characterized the amount of fixed charges contributing to the osmotic bending force using equilibrium swelling measurements conducted in water and in solutions of various NaCl concentrations. First we quantified the ionically active sodium acrylate groups in the gel after the polymerization. To that end, we took advantage of the fact that transition metals bind preferentially

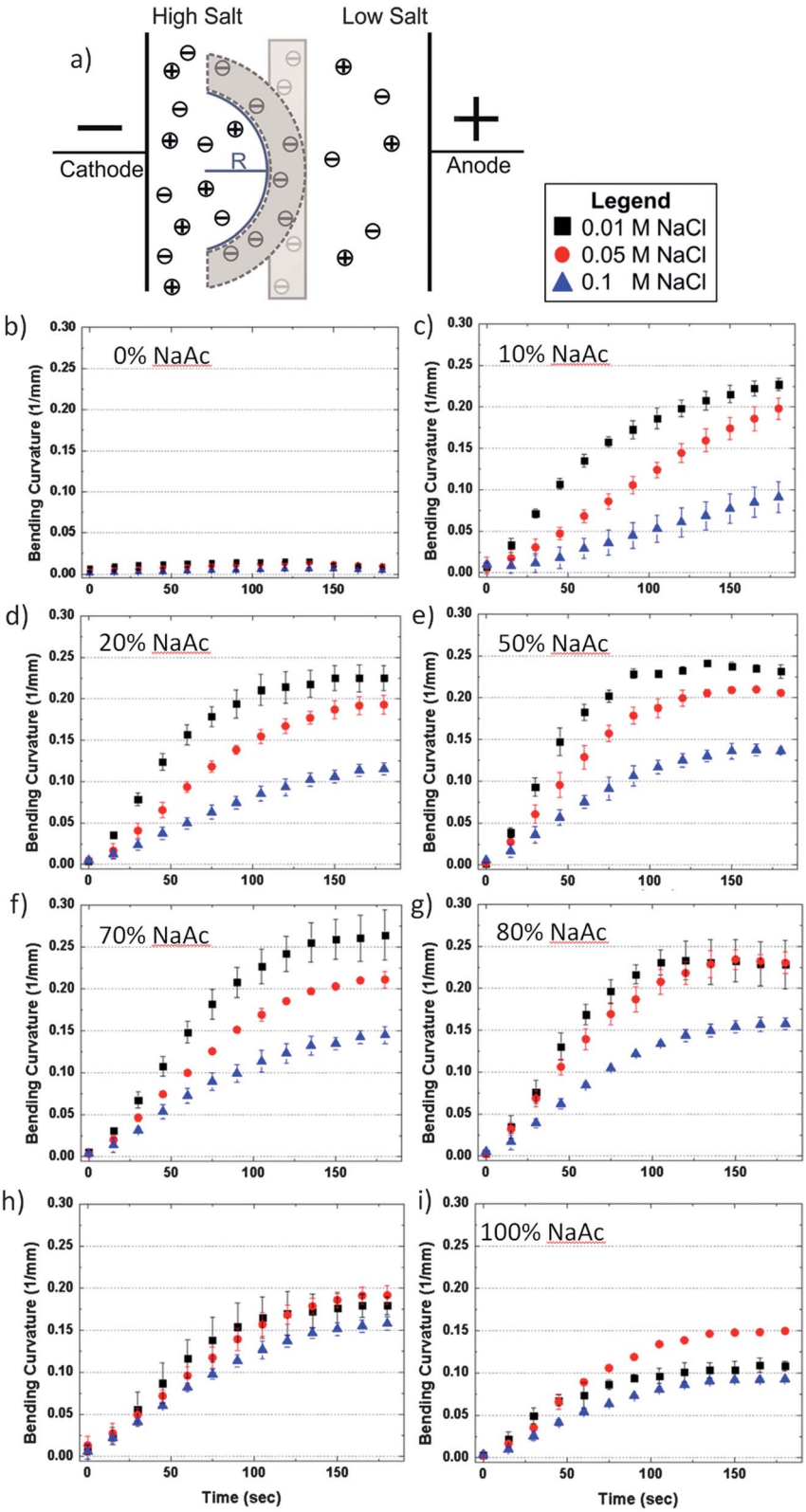

Fig. 4 The bending magnitude as a function of external salt concentration for each sodium acrylate/acrylamide gel composition. (a) Illustration of the mobile ion distribution for an anionic gel after application of an electric field. Higher osmotic pressure at the anode side of the gel drives bending toward the cathode. The radius of curvature is indicated by *R*. (b–i) The bending curvature as a function of applied electric field time in various NaCl solutions. The mole fraction of sodium acrylate in the gel network increases for each subsequent graph.

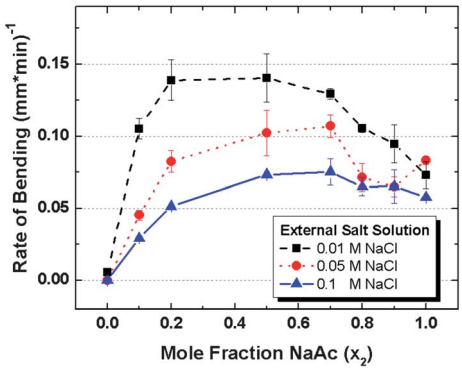

Fig. 5 Plot of the rate of increasing bending curvature as a function of the sodium acrylate content in the gel network after equilibration in 0.01 M, 0.05 M and 0.1 M NaCl. The maximum bending rate is achieved by anionic hydrogels composed with 50% sodium acrylate groups in 0.01 M NaCl.

to carboxylic groups due to their increased polarizability and ability to form ionic bridges.[55–57] We immersed the anionic gels in $CuSO_4$ to exchange the sodium counterions associated to the carboxylic groups with copper ions. We confirmed that the amount of fixed charge groups in the polymerized network is similar to that of the precursor solution. The concentration of sodium ions measured by inductively coupled plasma optical emission spectrometry (ICP-OES) measurements agrees very well with the expected bulk concentration of carboxylic groups in the gel (Fig. 6(a)).

Next, we characterized the swelling capacity of the various anionic networks, q_v, to obtain a qualitative measure of the contribution of the fixed charges to the osmotic swelling. We assumed that the extensibility of the various anionic gel networks is the same since we used a fixed concentration of monomer and crosslinker.[53] As shown in Fig. 6(b), the equilibrium swelling begins to plateau above a molar ratio of 50% NaAc. This result is either due to the limited extensibility of the polymer network, or "osmotically passive" counterions.

We sought to quantify the amount of fixed charge groups that should be ionized in the hydrogels of various compositions to achieve the measured equilibrium swelling in water using the Flory–Rehner[51,52,58] and Brannon–Peppas[59] theories. At equilibrium the total chemical potential gradient between the gel and external solution is minimized and can be expressed as the sum of the pressures due to polymer–solvent interactions (mix), the entropy change of the elongated polymer chains (el) and the non-uniform distribution of the mobile ions (ion):

$$\pi = \pi_{mix} + \pi_{el} + \pi_{ion} \quad (3)$$

The mixing contribution is given as:

$$\pi_{mix} = -\frac{RT}{V_1}\left(\ln(1-\nu_{2,s}) + \nu_{2,s} + \chi\nu_{2,s}^2\right) \quad (4)$$

where R is the gas constant, T is the temperature, χ is the solvent interaction parameter (0.48) and V_1 is the molar volume of the solvent (18 ml mol^{-1}).[54]

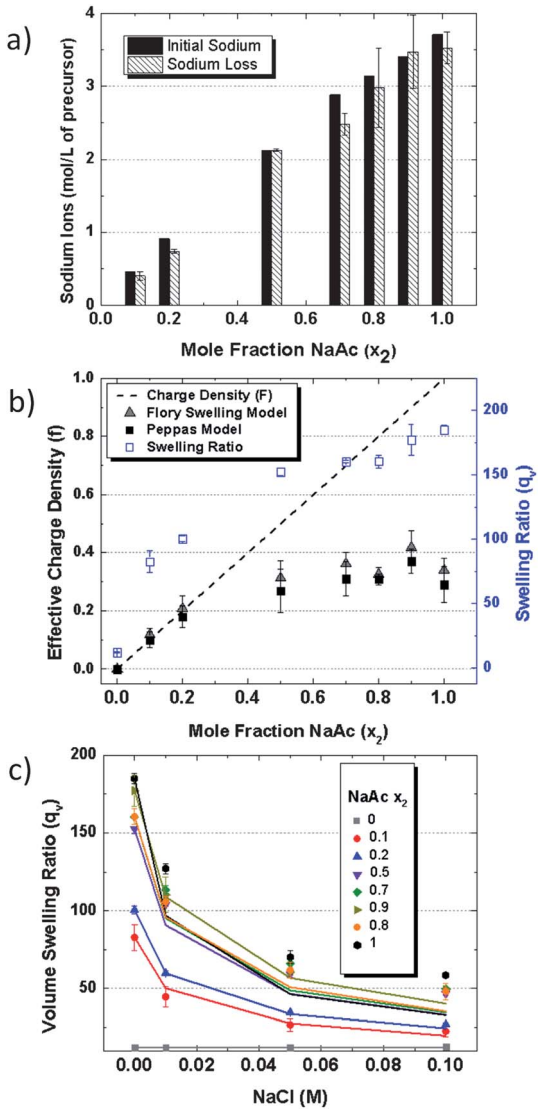

Fig. 6 (a) Plot of sodium ions initially in the gel and those expelled into a Cu_2SO_4 solution as a function of the gel composition. The good agreement indicates that the amount of sodium acrylate groups in the precursor solution is the same as in the polymerized gel. (b) Plot of the effective charge density (f) (calculated from eqn (8) and S4†) and equilibrium swelling ratio in water as a function of the gel composition. The dotted line represents the expected charge density (F) if all of the sodium acrylate groups present in the gel were ionized. The amount of effective charge groups begins to plateau past 50% NaAc (c) Plot of the measured (points) and calculated (lines) volume swelling ratios as a function of the external salt concentration. The ratios of effectively charged groups calculated from theory in water (f) were used to predict the gel swelling in salt solutions.

The elastic contribution, π_{el}, assuming that the network follows affine deformation,[58,60] is given by:

$$\pi_{el} = -\frac{RT}{V_1}N^{-1}\left[\nu_{2,s}^{1/3}\left(\nu_{2,r}^{2/3}\right) - \frac{\nu_{2,s}}{2}\right] \quad (5)$$

where N is the ratio of divinyl monomer units to crosslink units in the network. The ionic contribution π_{ion}, caused by the concentration difference of counterions between the gel and

solution is given by eqn (1). Donnan equilibrium and electroneutrality are satisfied for a system containing univalent salts when:

$$C_+^g C_-^g = C_+^s C_-^s = (C_{salt}^s)^2 \quad (6)$$

Due to the presence of fixed anions in the gel network, the amount of mobile cations in the gel is given as:

$$C_+^g = C_-^g + \frac{f}{V_r}\nu_{2,s} \quad (7)$$

where f is the molar ratio of effective fixed charge units in the gel network. The molar volume of the polymer repeat unit (V_r = 52.6 + 17.75F) was calculated using 71.08 g mol^{-1} and 95.06 g mol^{-1} for AAm and NaAc, respectively and the expected fixed charge density from the polymer precursor solution, F. Solving the set of equations to satisfy $\pi = 0$ at equilibrium yields the following equations, describing the equilibrium swelling of a gel network in aqueous salt solution:

$$\left(\ln(1-\nu_{2,s}) + \nu_{2,s} + \chi{\nu_{2,s}}^2\right) + N^{-1}\left[{\nu_{2,s}}^{1/3}{\nu_{2,r}}^{21/3} - \frac{\nu_{2,s}}{2}\right] - 2(K-1)V_1 C_{salt}^s - V_1\frac{f}{V_r}\nu_{2,s} = 0 \quad (8)$$

$$K\left(K + \frac{f\nu_{2,s}}{V_r C_{salt}^s}\right) - 1 = 0 \quad (9)$$

where $K = C_-^g/C_{salt}^s$ is the distribution coefficient of mobile ions between the gel and solution.[52]

The system of equations above was solved numerically in order to calculate the effective fixed charge density, f, of the gel networks at equilibrium. The dotted line in Fig. 6(b) represents the expected trend if all ionic groups present in the network were charged ($f = F$). The expected and effective charge densities are equal below 50% NaAc. Upon adding more fixed charges to the network, the effective charge density plateaus. Similar behavior has been observed for ionic hydrogel networks reported in literature.[47,51–54,61,62]

The plateau of effective fixed charges in Fig. 6(b) agrees well with the fixed charge density limit predicted by Manning for polyelectrolytes in aqueous solution.[63] According to Manning's theory, mobile ions form ion pairs with fixed charges along the polyelectrolyte chains at distances between two adjacent charges smaller than the Bjerrum length Q($Q = e^2/\varepsilon kT$), where e is the elementary charge, ε is the dielectric constant of the solvent and kT is the thermal energy contribution. The Bjerrum length is the scale where the electrostatic interaction energy of two charges in a medium is on the order of the thermal energy and the monomer size. At this scale, electrostatic attraction of the counterions for the fixed backbone overcomes the loss of translational entropy. At room temperature in water $Q \approx 0.71$ nm. For divinyl polymers the bond length between charge groups, b, can be estimated as 0.25 nm. Setting $Q = b/f$, the critical value of effective charge density is 36% which corresponds to the plateau observed in Fig. 6(b).

We evaluated the accuracy of the effective fixed charge densities calculated by the Flory–Rehner theory in predicting the gel swelling behavior with increasing salt content. The f values were fixed and the equilibrium swelling ratio was calculated and compared to measured values to confirm the accuracy of the calculated effective fixed charge values obtained for water. As shown in Fig. 6(c), the effective charge density values reasonably predict the gel swelling behavior in ionic solutions, with larger deviations at higher fixed charge values. While the calculated effective charge density, f, underestimates the swelling capacity for higher sodium acrylate content gels, the swelling capacity is greatly overestimated using the expected charge density values, F. It is evident that the formation of ion pairs at higher charge densities limits the magnitude of ionic gel bending during electro-actuation. However, quantitatively the plateau of 36% charge groups may not be accurate for a gel system. Manning's theory assumes rod-like polyelectrolytes in infinitely dilute solutions and does not take into account a crosslinked network where the mesh size may be on the order of neighboring charge distance. The calculation of the participating ionized groups was done for equilibrium conditions in water before application of an electric field and did not take into account the effect of mobilized ions on the effective fixed charge density. The effects of the mobile ions driven by the electric field on the degree of ionization and electrostatic interactions between the polymer chains were beyond the scope of this study.

Effect of mechanical properties on the bending curvature

While the charge density analysis provides insight as to why increasing charge density beyond a certain point can limit bending, it did not elucidate why the bending response of gel networks past the point of counterion condensation (>∼36% NaAc) differs from each other. We speculated that the continual lack of response of the gels with increased charge density may be a consequence of the mechanical properties of the gels. We conducted tensile extension tests of gels with various anionic compositions to analyze the effect of the modulus on the degree of bending as a function of the NaAc mole fraction (Fig. 7). The mechanics of gel bending in solution between parallel electrodes have previously been modeled as analogous to a bimetal, three point bending test:[4,35,39,45]

$$Y = \frac{L^2\sigma}{6WE} \quad (10)$$

where Y is the deflection of bending, W and L are the width and length of the beam respectively, E is the Young's Modulus and σ is the applied force. According to the above relationship the magnitude of gel bending should increase with a decrease in modulus.

Our results (Fig. 7) show an overall decrease in the Young's modulus with an increase in fixed charge density. As reported in the literature,[47,60,64–66] increasing the charge density of the gel

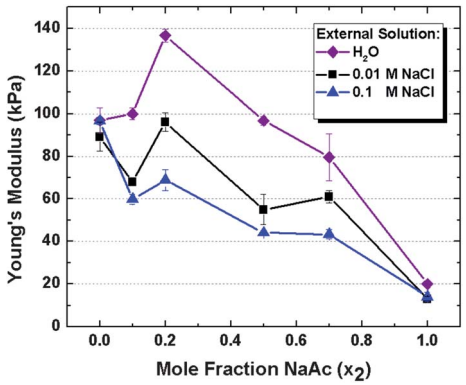

Fig. 7 Plot of Young's modulus as a function of the gel composition equilibrated in water, 0.01 M NaCl and 0.1 M NaCl. Overall, the modulus decreases with increasing fixed charge density, indicating that a lower modulus does not correspond to increased gel bending.

network should result in a decrease in modulus. However, the bending magnitude does not increase with a decrease in the Young's modulus as predicted by eqn (10). This may be due to the inability of the relationship to account for dynamic changes of electrostatic interactions within the gel network. This implies that the mechanical characteristics of the anionic networks do not affect greatly the bending magnitude within the modulus range. It is evident that the main factor driving the hydrogel electro-actuation is the osmotic pressure driven by the concentration difference of mobile ions between the gel and solution. The strength of the gel networks plays a secondary role.

Conclusions

We present gel actuators that can walk unidirectionally in dilute salt solutions without the need of ratcheted surfaces by using two legs composed of gels that deform in opposite directions to the electric field. The simple fabrication technique employs a laser writer that may enable mass production of oppositely charged gel appendages that can be "glued" temporarily in solution by the application of an electric field. Upon immersion in EDC, the gel walker components form permanent, covalent amide bonds at the cationic/anionic gel interface, which allow the walkers to operate completely submerged in aqueous solution.

We characterized the hydrogel networks in response to electric fields and the general swelling behavior in view of the walkers and other soft robotics applications. We found that the most responsive gel system contains the most ionized fixed charges (highest effective charge density, as opposed to the highest amount of NaAc) in a dilute salt solution to maximize the osmotic bending force, which is governed by the mobile ion difference between the gel and solution. When the external solution lacks mobile ions, bending is negligible. When the amount of overall fixed charges in the gel network is too high, mobile ions condense on the polymer backbone reducing the bending. We quantified the onset of the counterion condensation using the Flory–Rehner and Brannon–Peppas theories, which provided reasonable results and agreed well with the Manning's theory of counterion condensation. We also observed that the mechanical properties of the gel networks played a secondary role to the ionic interactions governing the bending.

Further studies will seek to elucidate the role of the electric field in dynamically promoting electrostatic shielding and counterion condensation during bending. Other ways of increasing the rate of response include changing factors such as the ionic path length of the walker legs and introducing porosity into the networks.[67] Since these gel walkers are operated in aqueous medium, the gel networks can easily be functionalized with biomolecules or other stimuli-responsive sensing elements. The results demonstrate a simple design strategy and biomimetic actuation mechanism that can be used to enable the use of soft robotics for sensing and transport applications.

Experimental

Materials

Anhydrous acrylic acid 99% (AAc, Sigma Aldrich), acrylamide (AAm, Sigma Aldrich), *N*,*N*′-methylenebis(acrylamide) (BAAm, Sigma Aldrich), ammonium persulfate (APS, Sigma Aldrich), *N*,*N*,*N*′*N*′-tetramethylethylenediamine 99.5% (TEMED, Sigma Aldrich), sodium hydroxide (Acros Chemical), copper(II) sulfate ($CuSO_4 \cdot 5H_2O$, Sigma Aldrich), sodium chloride (NaCl, Alfa Aesar), *N*,*N*-dimethylaminoethyl methacrylate (DMAEMA, Sigma), *N*,*N*-dimethylaminoethyl methacrylate "Q" Salt, methyl chloride (DMAEMA-Q, Dajac Labs), bromophenyl blue sodium salt (BPB, Acros Organics) and *N*-(3-dimethylaminopropyl)-*N*′-ethylcarbodiimide hydrochloride (EDC, Sigma Aldrich) were used as received. Sodium acrylate was prepared *in situ* by adding equimolar amounts of acrylic acid and sodium hydroxide to the precursor mixture. The gels were prepared and equilibrated in Milli-Q deionized water (18.2 MΩ cm).

Hydrogel polymerization

All hydrogels were prepared by thermal, free-radical polymerization in aqueous solution using BAAm as crosslinker. APS and TEMED were used as the initiator and accelerator, respectively.

For electro actuation curvature testing, the overall monomer concentration was fixed at 5 M and the crosslinker ratio (mole ratio of divinyl to vinyl monomers) was fixed at 1 : 200. The monomers were dissolved along with 67 μl of a 10 wt% APS solution in 5 ml of water. After addition of 25 μl of TEMED, the monomer solution was injected into Tygon tubing with 1.27 mm or 1.02 mm inner diameters. The hydrogel tubes were removed from a 70 °C oven after 1.5 hours and placed in an excess of Milli-Q water or the corresponding NaCl solution for at least one week before experimentation. For the gel walkers the DMAEMA-Q gels with a higher amount of crosslinker (1 : 100 crosslinker ratio) were made to obtain networks with a higher modulus.[68]

Gel sheets for tensile extension were formed by injecting NaAc/AAm and DMAEMA-Q/AAm solutions between glass slides

and PMMA substrates separated by 1 mm thick silicon spacers respectively. The molds for the thicker gel walker sheets were separated by 3 mm thick silicon spacers.

Gel walker fabrication

A laser writer (Universal Laser Systems VLS3.50) was used to cut arrays of gel appendages, designed using Corel Draw 10, to serve as the legs of the walker. The gels were cut after equilibration in 0.01 M NaCl at 88% power and 0.8% speed. After cutting, the gel pieces were placed in 0.01 M NaCl to re-equilibrate. The gels were electro-adhered by submerging the gel pieces in 0.01 M NaCl solution between two carbon electrodes. Attractive electrostatic interactions between the oppositely charged polymer networks were promoted by directionally applying an electric field (4 V cm^{-1}, 2 min) to promote interaction of the carboxylic and tertiary amine groups at the interface. After adhesion, the gel walkers were submerged in 10 mM EDC solution for 24 hours to promote covalent bond formation between the carboxylic and primary amine groups. Finally, the gel walkers were equilibrated in solutions of 0.01 M NaCl and 0.01 mM bromophenol blue in order to stain the cationic network for visualization.

Hydrogel equilibrium swelling

After polymerization, gel pieces were removed from Tygon tubing (1.27 mm inner diameter) and cut 20 mm in length. The mass and volume of each sample were recorded. The gel samples were then equilibrated in H_2O, 0.01 M NaCl, 0.05 M NaCl or 0.1 M NaCl for at least one week. After recording the mass and volume of each sample, the gels were dried in a vacuum oven at 80 °C until constant weight was reached. The weight swelling ratio after preparation, q_r, was calculated as:

$$q_r = \frac{\text{mass of gel after preparation}}{\text{mass of dry gel}} \tag{11}$$

The volume fraction of the polymer network after preparation, $v_{2,r}$, was calculated from the preparation weight swelling ratio as follows:

$$v_{2,r} = \left[1 + \frac{(q_r - 1)\rho}{d}\right]^{-1} \tag{12}$$

where ρ is the polymer density (1.35 g ml^{-1})[51–53,59] and d is the density of water (1 g ml^{-1}). The weight swelling ratio of hydrogels in water and in aqueous NaCl solutions, q_w, was calculated as:

$$q_w = \frac{\text{mass of gel after equilibration}}{\text{mass of dry gel}} \tag{13}$$

The volume fraction of the polymer network after equilibration, $v_{2,r}$, was calculated as:

$$v_{2,s} = \left[1 + \frac{(q_w - 1)\rho}{d}\right]^{-1} \tag{14}$$

The equilibrium volume swelling ratio, q_v, is reported as $1/v_{2,s}$. Each swelling ratio reported is an average of at least four separate measurements and the errors bars were calculated using the formula for standard deviation.

Electro-actuation

To isolate the effect of ionic interactions within the system on the gel bending, all parameters were kept constant while varying the internal polyelectrolyte (monomer ratio) and external salt concentration. To understand the electroactive behavior of gels initially at equilibrium, we equilibrated cylinders of hydrogel in salt solutions (0.01 M, 0.05 M, 0.1 M NaCl) before applying an electric field (3 V cm^{-1}) to the gel submerged in the corresponding solution. PDMS posts fixed the location of the gel between two graphite electrodes (5 cm apart) for 3 minutes before reversing the bias for another 3 min. Limiting the time range to 3 min prevented the pH gradient developed by electrolysis from reaching the gel and protonating the polymer backbone.[43] The radius of curvature as a function of time was recorded by analyzing pictures taken at 15 second intervals (Canon EOS Mark 2) with ImageJ software. We conducted initial experiments with gels of identical composition polymerized in 1.27 mm or 1.02 mm tubing in order to account for gel cylinders with varying diameters. It was found that the radius of curvature depends linearly on the thickness. All experimental bending data was normalized to a 2 mm gel cylinder diameter in order to account for the different thickness of the various gel compositions (see ESI for more details†). Each electro-actuation experiment was conducted at least three times and the error bars were calculated using the formula for standard deviation.

Mechanical testing

The mechanical properties of the hydrogels were measured by an Instron Model 5942 Tensile Tester, equipped with a 10 N load cell and 5 N pneumatic grips. Sand paper squares (1 × 1 cm) taped to the grips helped secure the hydrated gel networks. The Instron measured the lap shear adhesion strength (in extension mode at 1 mm min^{-1}) between the cationic and anionic networks in ambient atmosphere. Laser writer cut hydrated hydrogel samples (10 × 20 mm) were subsequently re-equilibrated in 0.01 M NaCl. The adhesion area was 3 × 9 mm and the approximate gel thickness was 3 mm. The adhesive shear strength was calculated as the maximum mechanical load/adhesion area. Each lap shear adhesion experiment was conducted at least three times and the errors bars were calculated using the formula for standard deviation.

The slope of the stress/strain curve within the region of 10% strain provided the Young's modulus for the various AAm/NaAc gels. Hydrated hydrogel samples were cut in a dog-bone shape according to ASTM D638-10 Type V (gage length = 7.62 mm, neck width = 3.18 mm)[69] with an approximate thickness of 3 mm. Gel samples were subsequently equilibrated in the solution of interest. A constant displacement rate of 3 mm min^{-1} was used. Each tensile extension experiment was conducted at least three times and the errors bars were calculated using the formula for standard deviation.

Charge density analysis

The Flory–Rehner[51,52,58] and Brannon–Peppas[59] theories were used to determine the amount of fixed charges contributing to the osmotic bending force within the pNaAc hydrogels (see ESI for more details†).

Inductively coupled plasma optical emission spectrometry (ICP-OES) measurements were conducted in order to verify that the gels contained the molar concentration of sodium acrylate groups present in the gel precursor solution. Gel samples were immersed in 0.01 M $CuSO_4$ solutions buffered with 0.1 M Tris (pH $\sim$ 9.0) to ensure the gel remained fully ionized (pK_a = 4.8).[52,66,70] We quantified the amount of sodium ions expelled from the gel network into the external solution after two weeks. At least four samples were characterized for each gel composition and the errors bars were calculated using the formula for standard deviation.

Acknowledgements

The support of this work by the Research Triangle NSF MRSEC on Programmable Soft Matter (DMR-1121107) and DS/DGA-France is gratefully acknowledged. We thank Kim Hutchison for her assistance with the ICP-OES measurements. We thank Dr Hanna Gracz for her assistance with the NMR experiments.

References

1 F. Ilievski, A. D. Mazzeo, R. F. Shepherd, X. Chen and G. M. Whitesides, *Angew. Chem., Int. Ed.*, 2011, **50**, 1890–1895.
2 R. F. Shepherd, F. llievski, C. Wonjae, M. A. Stephen, S. A. Stokes, M. D. Aaron, C. Xin, W. Michael and G. M. Whitesides, *Proc. Natl. Acad. Sci. U. S. A.*, 2011, **51**, 20400–20403.
3 M. Otake, Y. Kagami, M. Inaba and H. Inoue, *Robot. Auton. Syst.*, 2002, **40**, 185–191.
4 G. H. Kwon, G. H. Kwon, J. Y. Park, J. Y. Kim, L. F. Megan, D. J. Beebe and S. H. Lee, *Small*, 2008, **4**, 2148–2153.
5 X. He, H. Ximin, M. Aizenberg, O. Kuksenok, L. D. Zarzar, A. Shastri, A. C. Balazs and J. Aizenberg, *Nature*, 2012, **487**, 214–218.
6 Z. L. Wu, M. Moshe, J. Greener, H. Therien-Aubin, Z. Nie, E. Sharon and E. Kumacheva, *Nat. Commun.*, 2013, **4**, 1586.
7 E. P. Palleau, D. Morales, M. D. Dickey and O. D. Velev, *Nat. Commun.*, 2013, **4**, 2257.
8 J. Kim, B. Kim, J. Ryu, Y. Jeong, J. Park, H. C. Kim and K. Chun, *Jpn. J. Appl. Phys., Part 1*, 2005, **44**, 5764–5768.
9 L. Yeghiazarian, H. Arora, V. Nistor, C. Montemagno and U. Wiesner, *Soft Matter*, 2007, **3**, 939.
10 P. Techawanitchai, M. Ebara, N. Idota, T. A. Asoh, A. Kikuchi and T. Aoyagi, *Soft Matter*, 2012, **8**, 2844–2851.
11 L. Mahadevan, S. Daniel and M. K. Chaudhury, *Proc. Natl. Acad. Sci. U. S. A.*, 2004, **101**, 23.
12 H. Lee, C. Xia and N. X. Fang, *Soft Matter*, 2010, **6**, 4342–4345.
13 V. Chan, K. Park, M. B. Collens, H. Kong, T. A. Saif and R. Bashir, *Sci. Rep.*, 2012, **2**, 857.
14 S. Maeda, Y. Hara, T. Sakai, R. Yoshida and S. Hashimoto, *Adv. Mater.*, 2007, **19**, 3480–3484.
15 S. Maeda, Y. Hara, S. Nakamaru and S. Hashimoto, *Polymers*, 2011, **3**, 299–313.
16 P. Dayal, O. Kuksenok and A. C. Balazs, *Soft Matter*, 2010, **6**, 768–773.
17 F. Horkay, I. Tasaki and P. J. Basser, *Biomacromolecules*, 2000, **2**, 195–199.
18 Y. Osada, H. Okuzaki and H. Hori, *Nature*, 1992, **355**, 242–244.
19 M. Otake, M. Inaba and H. Inoue, *Robot. Autom. 2000 Proc. ICRA 2000 IEEE Int. Conf.*, 2000, **1**, 488–493.
20 S. Liang, J. Xu, L. Weng, L. Zhang, X. Guo and X. Zhang, *J. Polym. Sci., Part B: Polym. Phys.*, 2007, **45**, 1187–1197.
21 T. Shiga, *Neutron Spin Echo Spectrosc. Viscoelasticity Rheol.*, 1997, vol.134, pp. 131–163.
22 Y. Ma, Y. Zhang, B. Wu, W. Sun, Z. Li and J. Sun, *Angew. Chem., Int. Ed.*, 2011, **50**, 6254–6257.
23 B. Yıldız, B. Işık, M. Kış and Ö. Birgül, *J. Appl. Polym. Sci.*, 2003, **88**, 2028–2031.
24 A. Phadke, A. Phadkea, C. Zhanga, B. Armanb, C. C. Hsuc, R. A. Mashelkard, A. K. Leled, M. J. Tauberc, G. Aryab and S. Varghese, *Proc. Natl. Acad. Sci. U. S. A.*, 2012, **109**, 4383–4388.
25 G. Sudre, L. Olanier, Y. Tran, D. Hourdet and C. Creton, *Soft Matter*, 2012, **8**, 8184–8193.
26 D. Sakasegawa, M. Goto and A. Suzuki, *Colloid Polym. Sci.*, 2009, **287**, 1281–1293.
27 A. Harada, R. Kobayashi, Y. Takashima, A. Hashidzume and H. Yamaguchi, *Nat. Chem.*, 2011, **3**, 34–37.
28 T.-A. Asoh and A. Kikuchi, Electrophoretic adhesion of stimuli-responsive hydrogels, *Chem. Commun.*, 2010, **46**, 7793.
29 T. A. Asoh, W. Kawai and A. Kikuchi, *Soft Matter*, 2012, **8**, 1923.
30 R. D. Ratner, in *Hydrogels in Medicine and Pharmacy: Fundamentals*, ed. N. A. Peppas, CRC Press, Boca Raton, 1986, vol. 1, ch. 4, pp. 85–94.
31 N. A. Peppas and E. W. Merrill, *J. Appl. Polym. Sci.*, 1977, **21**, 1763–1770.
32 T. Tominaga, T. Kurokawa, H. Furukawa, Y. Osada and J. P. Gong, *Soft Matter*, 2008, **4**, 1645–1652.
33 E. Jabbari, J. Tavakoli and A. S. Sarvestani, *Smart Mater. Struct.*, 2007, **16**, 1614–1620.
34 D. E. De Rossi, P. Chiarelli, G. Buzzigoli, C. Domenici and L. Lazzeri, *Trans. - Am. Soc. Artif. Intern. Organs*, 1986, **32**, 157–162.
35 T. Shiga and T. Kurauchi, *J. Appl. Polym. Sci.*, 1990, **39**, 2305–2320.
36 M. Doi, M. Matsumoto and Y. Hirose, *Macromolecules*, 1992, **25**, 5504–5511.
37 T. Shiga, Y. Hirose, A. Okada and T. Kurauchi, *J. Appl. Polym. Sci.*, 1993, **47**, 113–119.
38 T. Tanaka, I. Nishio, S. T. Sun and S. Ueno-Nishio, *Science*, 1982, **218**, 467–469.
39 I. C. Kwon, Y. H. Bae and S. W. Kim, *J. Polym. Sci., Part B: Polym. Phys.*, 1994, **32**, 1085–1092.

40 M. Homma, Y. Seida and Y. Nakano, *J. Appl. Polym. Sci.*, 2000, **75**, 111–118.
41 X. Zhou, Y. C. Hon, S. Sun and A. F. T. Mak, *Smart Mater. Struct.*, 2002, **11**, 459–467.
42 M. J. Bassetti, A. N. Chatterjee, N. R. Aluru and D. J. Beebe, *J. Microelectromech. Syst.*, 2005, **14**, 1198–1207.
43 P. J. Glazer, M. van Erp, A. Embrechts, S. G. Lemay and E. Mendes, *Soft Matter*, 2012, **8**, 4421–4426.
44 G. Pollack, in *Cells, Gels and the Engines of Life*, Ebner and Sons, South Korea, 2001, pp. 87–109.
45 G. Liu and X. Zhao, *J. Macromol. Sci., Part A: Pure Appl.Chem.*, 2005, **42**, 51–59.
46 S. Sun and A. F. T. Mak, *J. Polym. Sci., Part B: Polym. Phys.*, 2001, **39**, 236–246.
47 R. Skouri, F. Schosseler, J. P. Munch and S. J. Candau, *Macromolecules*, 1995, **28**, 197–210.
48 J. Fei, Z. Zhang and L. Gu, *Polym. Int.*, 2002, **51**, 502–509.
49 T. Shiga, Y. Hirose, A. Okada and T. Kurauchi, *J. Appl. Polym. Sci.*, 1992, **44**, 249–253.
50 K. B. Zeldovich and A. R. Khokhlov, *Macromolecules*, 1999, **32**, 3488–3494.
51 S. Durmaz and O. Okay, *Polymer*, 2000, **41**, 3693–3704.
52 O. Okay and S. B. Sariisik, *Eur. Polym. J.*, 2000, **36**, 393–399.
53 M. Silberberg-Bouhnik, O. Ramon, I. Ladyzhinski, S. Mizrahi and Y. Cohen, *J. Polym. Sci., Part B: Polym. Phys.*, 1995, **33**, 2269–2279.
54 J. Baker, L. Hong, H. Blanch and J. Prausnitz, *Macromolecules*, 1994, **27**, 1446–1454.
55 W. Li, H. Zhao, P. Teasdale, R. John and S. Zhang, *React. Funct. Polym.*, 2002, **52**, 31–41.
56 H. P. Gregor, L. B. Luttinger and E. M. Loebl, *J. Phys. Chem.*, 1955, **59**, 34–39.
57 F. T. Wall and S. J. Gill, *J. Phys. Chem.*, 1954, **58**, 1128–1130.
58 P. J. Flory, in *Principles of Polymer Chemistry*, Cornell University Press, Ithaca, 1953, pp. 584–594.
59 L. Brannon-Peppas and N. A. Peppas, *Chem. Eng. Sci.*, 1991, **46**, 715–722.
60 G. Nisato, R. Skouri, F. Schosseler, J. P. Munch and S. J. Candau, *Faraday Discuss.*, 1995, **101**, 133–146.
61 S. Bajpai and S. Johnson, *React. Funct. Polym.*, 2005, **62**, 271–283.
62 X. Liu, Z. Tong and O. Hu, *Macromolecules*, 1995, **28**, 3813–3817.
63 G. S. Manning, *J. Chem. Phys.*, 1969, **51**, 924–933.
64 M. Rubinstein, R. H. Colby, A. V. Dobrynin and J. F. Joanny, *Macromolecules*, 1996, **29**, 398–406.
65 O. Okay and S. Durmaz, *Polymer*, 2002, **43**, 1215–1221.
66 B. A. Baker, R. L. Murff and V. T. Milam, *Polymer*, 2010, **51**, 2207–2214.
67 M. L. O'Grady, P. Kuo and K. K. Parker, *ACS Appl. Mater. Interfaces*, 2009, **2**, 343–346.
68 C. Uzun, M. Hassnisaber, M. Şen and O. Güven, *Nucl. Instrum. Methods Phys. Res., Sect. B*, 2003, **208**, 242–246.
69 ASTM D 638-10, *Standard Test Method for Tensile Properties of Plastics*, ASTM International, West Conshohocken, PA, 2010.
70 K. El Brahmi, M. Rawiso and J. François, *Eur. Polym. J.*, 1993, **29**, 1531–1537.